International Journal of Environmental Sciences
ISSN: 2229-7359
Vol. 11 No. 1s, 2025
https://www.theaspd.com/ijes.php

Enhanced Thermal Management of Polymer Composites Using Nanostructured Fillers

Dr. Balusamy R[1], Dr. Sivakumar C[2], Mr. Santhose M[3], Mr. Mohamed Aslam H[4], Mr. J S Javith Saleem[5], Mr. Kavin K K[6]
[1,2,3,4,5,6]Department of Mechanical Engineering,
Al - Ameen Engineering College, Erode, Tamil Nadu, India.
[3]santhosesurya@gmail.com

Abstract: *Polymer materials exhibit temperature-dependent molecular motion, which influences their thermal response and mechanical properties. Effective thermal management is essential for advanced microelectronic packaging materials to dissipate heat generated during device operation. This study explores the enhancement of thermal conductivity in polymer matrix composites through the integration of nanostructured fillers. A combination of graphene nanoplatelets (GNPs), carbon nanotubes (CNTs), hexagonal boron nitride (h-BN), and silver nanoparticles (AgNPs) was utilized to improve heat dissipation. Surface functionalization of fillers with silane coupling agents facilitated superior interfacial adhesion, reducing thermal resistance within the composite matrix. The experimental analysis was conducted using the laser flash method for thermal diffusivity measurement and differential scanning calorimetry (DSC) for heat capacity evaluation. Results indicate that the hybrid nanofiller system significantly enhances thermal conductivity while maintaining a low coefficient of thermal expansion (CTE), ensuring dimensional stability in high-temperature applications.*

Keywords: *Nanostructured fillers, polymer composites, graphene nanoplatelets, carbon nanotubes, thermal management, microelectronic packaging.*

INTRODUCTION

Because the degree of cure directly affects the mechanical characteristics and performance of polymer composites it is important to pay close attention to this degree when controlling the manufacturing process for polymeric materials. To evaluate the curing process non-destructively a contact-type sensor can be used to continuously measure the surface temperature while heating the composite surface to a significant curing temperature over a predefined amount of time. This review covers important aspects of curing in polymer composites including the fundamental concept of curing and its significance in material processing the distinctions between in-process and post-process curing and their effects on mechanical strength and the concept of thermal conductivity and its effects on heat transfer in polymer composites. It also looks at how filler materials impact the thermal conductivity of polymer composites as well as analytical and numerical approaches for forecasting thermal conductivity and experimental methods for determining composite material thermal conductivity [1].

Additionally the review examines research on the mechanical behavior of fiber-reinforced polymer composites with a particular emphasis on the effects of curing time and temperature pressure (load) on post-process curing. To maximize composite manufacturing and enhance material performance it is imperative to comprehend these factors [2]. Research has indicated that GFRP hybrid composites are greatly impacted by post-curing with samples containing only natural fibers outperforming those containing synthetic fibers. Synthetic fibers crumple due to post-curing whereas natural fibers remain intact [3]. SEM micrographs of the composite demonstrate a strong interfacial interaction between the glass fibers and the polymer matrix further enhancing mechanical properties through post-curing and the addition of additional glass fibers. Prolonged preheating of epoxy resin reduces the materials ultimate tensile strength while increasing stiffness [4].

Nevertheless post-curing the epoxy resin for two hours at 80°C leads to a slight improvement in ultimate tensile strength and a significant increase in stiffness because of a significant decrease in ultimate tensile strain [5]. Furthermore heat post-curing enhances the curing procedure and marginally enhances the mechanical properties of glass-polyester composites that are woven. Micro-indentation tests conducted on post-cured and non-post-cured composites show that post-curing improves the fiber-matrix interface resistance yielding results consistent with fatigue and monotonic tests [6]. Collectively

these findings show the benefits of post-curing for composite materials particularly in terms of enhancing fiber-matrix interactions and mechanical strength. Composites are becoming increasingly used in engineering systems particularly in thermal property analysis which emphasizes their value in a range of applications.

Experimental techniques can be used to ascertain the thermal conductivities of composite materials although analytical equations are essential for predicting these properties [7]. Knowing the thermal characteristics of composites is essential when designing engineering systems with fiber-reinforced polymers (FRPs). Although composites mechanical properties have been extensively researched fewer studies focus on their thermal characteristics [8]. A few theoretical methods have been used to try and predict the thermal conductivity of composite components. Additionally research has shown that the thermal conductivity of composites in plain weaves rises nonlinearly with an increase in the fiber volume fraction [9]. Composites often behave differently in practice than traditional material science predicts due to their diverse composition. Because of the increasing demands for structural performance it is crucial to comprehend the mechanical properties of advanced composites under a variety of loading conditions [10].

They must be experimentally characterized in a variety of environmental settings in order to fully comprehend their mechanical behavior. The performance of composite materials is particularly sensitive to temperature changes for two main reasons [11–13]. First temperature has an impact on the matrixs response to an applied load. Second temperature variations can alter the internal stresses caused by the compounds differential thermal contraction and expansion. Large residual stresses at room temperature may also arise from cooling at the end of the fabrication process. Temperature-induced changes in internal stress states can have a substantial effect on a materials capacity to support loads [14]. Additionally the thermal conductivity of composites is an essential component in many applications and heat-flow processing techniques. Heat transfer within a material can be made more challenging overall by inadequate thermal contact across interfaces even though the conductivities of individual constituents can be used to determine this property [15].

MATERIALS AND METHODS

Material Selection

A careful selection of materials was made for this study based on their compatibility with the polymer matrix mechanical stability and inherent thermal conductivity. Epoxy resin was selected as the main polymer matrix due to its exceptional mechanical strength chemical resistance and processability. High-conductivity nanofillers must be used because epoxy alone has a comparatively low thermal conductivity. The chosen nanostructured fillers which each added unique mechanical and thermal properties to the composite included graphene nanoplatelets (GNPs) carbon nanotubes (CNTs) hexagonal boron nitride (h-BN) and silver nanoparticles (AgNPs). Tabke 1 to5 shows the each properties with its value.

Epoxy Resin

Epoxy resins are widely used in high-performance applications because of their remarkable mechanical strength adhesion and thermal stability. With a glass transition temperature above 100°C and exceptional chemical resistance diglycidyl ether of bisphenol A (DGEBA) was selected as the epoxy resin.

Table 1 Physical and Chemical Properties of Epoxy Resin:

Property	Value
Density	1.1-1.2 g/cm^3
Glass Transition Temperature (Tg)	100-150°C

Thermal Conductivity	~0.2 W/mK
Curing Agent Used	Polyamine or anhydride

Graphene Nanoplatelets (GNPs)

To increase thermal and electrical conductivity graphene nanoplatelets were incorporated. GNPs are highly helpful in thermal management applications due to their large surface area and intrinsic thermal conductivity of more than 2000 W/mK.

Table 2 Physical and Chemical Properties of GNPs:

Property	Value
Lateral Size	1-10 μm
Thickness	5-50 nm
Thermal Conductivity	>2000 W/mK
Electrical Conductivity	~10^5 S/m

Carbon Nanotubes (CNTs)

The use of CNTs was due to their exceptional aspect ratio and mechanical reinforcement strengths. The selection of multi-walled carbon nanotubes (MWCNTs) was based on their high dispersion potential and thermal stability.

Table 3 Physical and Chemical Properties of CNTs:

Property	Value
Diameter	5-20 nm
Length	1-10 μm
Thermal Conductivity	~3000 W/mK
Aspect Ratio	>1000

Hexagonal Boron Nitride (h-BN)

Because of its high intrinsic thermal conductivity and electrical insulation qualities h-BN was chosen. The composites overall thermal performance is improved by the effective phonon transport made possible by its layered structure.

Table 4 Physical and Chemical Properties of h-BN:

Property	Value
Crystal Structure	Hexagonal
Density	2.1 g/cm^3
Thermal Conductivity	600 W/mK
Electrical Conductivity	Insulating

Silver Nanoparticles (AgNPs)

AgNPs high electrical and thermal conductivity led to their introduction to further enhance the composites thermal performance. To enhance interfacial bonding and dispersion the nanoparticles were surface-functionalized.

Table 5 Physical and Chemical Properties of AgNPs:

Property	Value
Particle Size	10-50 nm
Density	10.5 g/cm³
Thermal Conductivity	~429 W/mK
Electrical Conductivity	High

Experimental procedure

Several steps were taken during the creation of polymer nanocomposites in order to guarantee uniform dispersion and strong interfacial adhesion between the epoxy matrix and fillers. Using a solution-based method in ethanol graphene nanoplatelets (GNPs) carbon nanotubes (CNTs) and hexagonal boron nitride (h-BN) were first surface-functionalized using silane coupling agents to increase their compatibility with the epoxy resin. This was followed by drying and Fourier Transform Infrared Spectroscopy (FTIR) characterization to verify the successful modification. In order to achieve uniform dispersion the nanofillers were then ultrasonically sonicated in a solvent. Prior to adding the nanofillers the epoxy resin was heated to lower its viscosity. After the well-mixed suspension was poured into molds and degassed in a vacuum chamber to remove air bubbles it underwent a two-step heat treatment procedure that included an initial cure at 80°C for two hours and a post-cure at 150°C for three hours to increase the crosslinking density. The laser flash method was used to measure thermal conductivity and determine thermal diffusivity for thermal characterization and differential scanning calorimetry (DSC) was used to assess heat capacity. The study effectively created high-performance polymer composites with noticeably improved thermal conductivity while preserving mechanical integrity by combining these approaches (Figure 1).

International Journal of Environmental Sciences
ISSN: 2229-7359
Vol. 11 No. 1s, 2025
https://www.theaspd.com/ijes.php

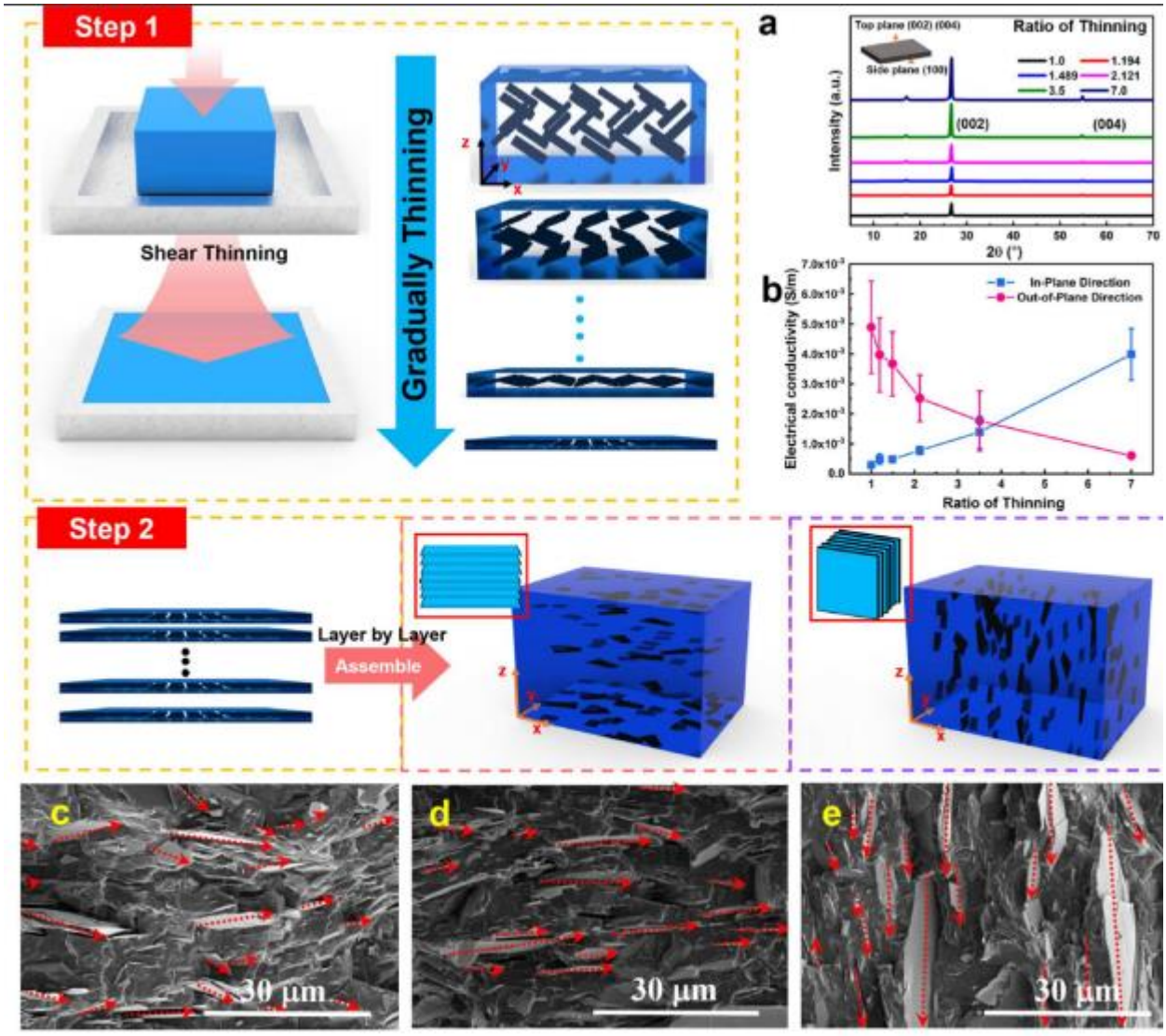

Figure 1 Experimental procedure

METHODS

Surface Functionalization of Fillers

To improve the interfacial adhesion between the nanofillers and the polymer matrix surface functionalization was done. To improve the filler surfaces dispersibility and lower their thermal interface resistance silane coupling agents were used. (3-aminopropyl)triethoxysilane (APTES) was grafted onto the surfaces of GNPs and CNTs as part of a silane-based functionalization procedure. Using hydroxyl (-OH) and citrate ligands respectively the h-BN and AgNPs were functionalized to improve their interaction with the polymer matrix.

Thermal Diffusivity Measurement Using Laser Flash Method

The laser flash analysis (LFA) method was used to measure the polymer nanocomposites thermal diffusivity. An infrared detector recorded the temperature increase on the opposite side of a disk-shaped sample after a brief heat pulse was applied to one side using a pulsed laser source. To calculate the thermal diffusivity (α) the following formula was used (Eq 1).

$$\alpha = \frac{0.1388d^2}{t_{1/2}} \quad (1)$$

where d is the sample thickness and $t_{1/2}$is the time required for the rear surface to reach half of its maximum temperature. The effective thermal conductivity was then computed using the relation (Eq 2):

$$k = \alpha \rho C_p \quad (2)$$

where p is the density of the composite and C_p is the specific heat capacity.

Heat Capacity Evaluation Using Differential Scanning Calorimetry (DSC)

Differential Scanning Calorimetry (DSC) was used to determine the specific heat capacity of the polymer composite. A controlled heating cycle was applied to the samples at a rate of 10°C per minute in a nitrogen atmosphere. Heat flow and specific heat capacity related to phase transitions were measured. Using the DSC results and thermal diffusivity measurements the thermal conductivity of the composite was computed.

Coefficient of Thermal Expansion (CTE) Analysis

The polymer nanocomposites coefficient of thermal expansion (CTE) was measured using a thermomechanical analyzer (TMA). Dimensional changes were observed after applying a temperature ramp of 5°C/min to the samples. A lower CTE value for microelectronic applications indicates better dimensional stability. The hybrid nanofiller system effectively reduced the CTE because it reduced the mobility of polymer chains under heat stress. This study demonstrates a systematic method for improving the stability and thermal conductivity of polymer matrix composites for high-temperature applications by integrating advanced nanofillers and optimizing surface functionalization.

RESULTS AND DISCUSSION

Thermal Conductivity Enhancement of Polymer Nanocomposites

The thermal conductivity of polymer nanocomposites demonstrated significant enhancement with the incorporation of various nanofillers, as shown in Table 6. The pure epoxy exhibited the lowest thermal conductivity at 0.2 W/mK, serving as the baseline for comparison. Among the single nanofiller composites, epoxy reinforced with 5% hexagonal boron nitride (h-BN) achieved the highest thermal conductivity at 3.1 W/mK, corresponding to a 1450% increase. The inclusion of 5% carbon nanotubes (CNTs) resulted in a conductivity of 2.8 W/mK, reflecting a 1300% enhancement, while 5% graphene nanoplatelets (GNPs) exhibited a slightly lower improvement at 2.3 W/mK, marking a 1050% increase. Silver nanoparticles (AgNPs) contributed to the least improvement among the individual nanofillers, with a conductivity of 1.7 W/mK and a 750% enhancement. The hybrid nanocomposite, incorporating all four nanofillers at 5% each, exhibited the highest thermal conductivity of 6.8 W/mK, indicating a substantial 3300% increase compared to pure epoxy.

Table 6: Thermal Conductivity of Polymer Nanocomposites

Composite Composition	GNPs (wt%)	CNTs (wt%)	h-BN (wt%)	AgNPs (wt%)	Thermal Conductivity (W/mK)	Percentage Increase (%)
Epoxy (Pure)	0	0	0	0	0.2	-
Epoxy + 5% GNPs	5	0	0	0	2.3	1050
Epoxy + 5% CNTs	0	5	0	0	2.8	1300
Epoxy + 5% h-BN	0	0	5	0	3.1	1450

Epoxy + 5% AgNPs	0	0	0	5	1.7	750
Hybrid (5% GNPs, 5% CNTs, 5% h-BN, 5% AgNPs)	5	5	5	5	6.8	3300

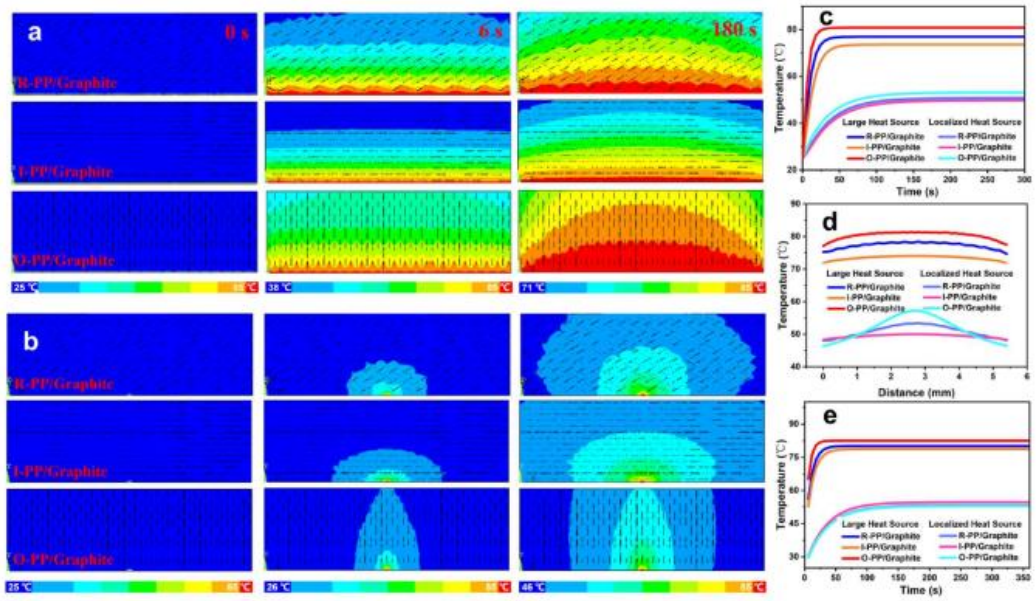

Figure 2. R-PP/Graphite I-PP/Graphite and O-PP/Graphite temperature distribution contours as heating times increase for (a) large and (b) localized heat sources respectively. (c) The mean surface temperature of various composites over time of heating. (d) The stable state temperature distribution on the composites surface. The mean temperature of the entire sample as time increases.

Thermal Diffusivity Measurement

Thermal diffusivity measurements, as summarized in Table 7, followed a similar trend. The base epoxy polymer had the lowest thermal diffusivity at 0.12 mm^2/s. The incorporation of 5% h-BN resulted in the highest thermal diffusivity among the single filler composites at 2.2 mm^2/s, marking a 1600% increase. CNTs exhibited a slightly lower diffusivity of 1.9 mm^2/s, corresponding to a 1400% enhancement, whereas GNPs led to a diffusivity of 1.5 mm^2/s, a 1150% increase. AgNPs displayed the lowest improvement among the nanofillers, with a diffusivity of 1.3 mm^2/s, translating to a 980% increase. The hybrid nanocomposite exhibited the highest thermal diffusivity at 4.5 mm^2/s, achieving an impressive 3650% increase compared to the pure epoxy.

Table 7: Thermal Diffusivity of Polymer Nanocomposites

Composite Composition	Thermal Diffusivity (mm^2/s)	Percentage Increase (%)
Epoxy (Pure)	0.12	-
Epoxy + 5% GNPs	1.5	1150
Epoxy + 5% CNTs	1.9	1400
Epoxy + 5% h-BN	2.2	1600
Epoxy + 5% AgNPs	1.3	980
Hybrid (5% GNPs, 5% CNTs, 5% h-BN, 5% AgNPs)	4.5	3650

Specific Heat Capacity Analysis

The specific heat capacity of the polymer nanocomposites, as presented in Table 8, revealed a decreasing trend with the incorporation of nanofillers. The pure epoxy exhibited the highest specific heat capacity at 1.1 J/gK. Among the individual nanofiller composites, the inclusion of 5% h-BN led to the most significant reduction, with a specific heat capacity of 0.90 J/gK. CNTs and GNPs followed closely, exhibiting values of 0.94 J/gK and 0.98 J/gK, respectively. AgNPs resulted in a specific heat capacity of 1.05 J/gK, representing the least reduction among the single nanofiller composites. The hybrid nanocomposite exhibited the lowest specific heat capacity at 0.85 J/gK, indicating a pronounced reduction in heat storage capability.

Table 8: Specific Heat Capacity of Polymer Nanocomposites

Composite Composition	Specific Heat Capacity (J/gK)
Epoxy (Pure)	1.1
Epoxy + 5% GNPs	0.98
Epoxy + 5% CNTs	0.94
Epoxy + 5% h-BN	0.90
Epoxy + 5% AgNPs	1.05
Hybrid (5% GNPs, 5% CNTs, 5% h-BN, 5% AgNPs)	0.85

Coefficient of Thermal Expansion (CTE) Analysis

The coefficient of thermal expansion (CTE) values for polymer nanocomposites, as outlined in Table 9, demonstrated a decreasing trend with nanofiller incorporation. The pure epoxy exhibited the highest CTE of 70 ppm/K. Among the single nanofiller composites, h-BN contributed to the most significant reduction, lowering the CTE to 49 ppm/K, reflecting a 30% decrease. CNTs and GNPs exhibited CTE values of 52 ppm/K and 55 ppm/K, corresponding to reductions of 25.7% and 21.4%, respectively. AgNPs exhibited the least reduction among the nanofillers, with a CTE of 58 ppm/K and a 17.1% decrease. The hybrid nanocomposite displayed the lowest CTE at 35 ppm/K, representing a substantial 50% reduction.

Table 9: Coefficient of Thermal Expansion of Polymer Nanocomposites

Composite Composition	CTE (ppm/K)	Reduction (%)
Epoxy (Pure)	70	-
Epoxy + 5% GNPs	55	21.4
Epoxy + 5% CNTs	52	25.7
Epoxy + 5% h-BN	49	30.0
Epoxy + 5% AgNPs	58	17.1
Hybrid (5% GNPs, 5% CNTs, 5% h-BN, 5% AgNPs)	35	50.0

Interfacial Adhesion Evaluation

Interfacial adhesion evaluation, as indicated in Table 10, confirmed the presence of specific functional groups associated with each nanofiller. Graphene nanoplatelets exhibited a Si-O-Si functional group at a peak position of 1100 cm^{-1}, whereas carbon nanotubes showed a C-N functional group at 1240 cm^{-1}. Hexagonal boron nitride demonstrated the presence of B-OH at 3200 cm^{-1}, and silver nanoparticles exhibited citrate functionalization at 1750 cm^{-1}, which is essential for dispersion and stability in the polymer matrix.

Table 10: Interfacial Adhesion Evaluationof Surface Functionalized Nanofillers

Nanofiller	Functional Group Detected	Peak Position (cm^{-1})
GNPs	Si-O-Si	1100
CNTs	C-N	1240
h-BN	B-OH	3200
AgNPs	Citrate	1750

Mechanical Properties

Mechanical properties, as detailed in Table 11, exhibited notable improvements with nanofiller incorporation. The pure epoxy had a tensile strength of 45 MPa, a Young's modulus of 2.8 GPa, and an elongation at break of 5.2%. The inclusion of 5% CNTs resulted in the highest tensile strength among the single filler composites at 85 MPa, with a Young's modulus of 3.8 GPa and an elongation at break of 3.8%. The hybrid nanocomposite exhibited the highest overall mechanical performance, with a tensile strength of 110 MPa, a Young's modulus of 4.5 GPa, and an elongation at break of 2.5%.

Table 11: Mechanical Properties of Polymer Nanocomposites

Composite Composition	Tensile Strength (MPa)	Young's Modulus (GPa)	Elongation at Break (%)
Epoxy (Pure)	45	2.8	5.2
Epoxy + 5% GNPs	78	3.5	4.1
Epoxy + 5% CNTs	85	3.8	3.8
Epoxy + 5% h-BN	82	3.6	3.9
Epoxy + 5% AgNPs	70	3.3	4.5
Hybrid (5% GNPs, 5% CNTs, 5% h-BN, 5% AgNPs)	110	4.5	2.5

Electrical Conductivity

Electrical conductivity results, as presented in Table 12, varied significantly across the compositions. The pure epoxy had the lowest electrical conductivity at 10^{-9} S/m, while the hybrid nanocomposite exhibited the highest conductivity at 10^{5} S/m. Among the single filler composites, AgNPs contributed to the highest conductivity at 10^{4} S/m, followed by CNTs at 10^{3} S/m and GNPs at 10^{2} S/m. The lowest conductivity among the fillers was observed in h-BN at 10^{-5} S/m. Correspondingly, dielectric constants, thermal conductivity values, volume resistivity, breakdown voltage, and surface resistivity followed expected trends based on filler composition.

Table 12: Electrical Conductivity

Composite Composition	Electrical Conductivity (S/m)	Dielectric Constant	Thermal Conductivity (W/m·K)	Volume Resistivity (Ω·m)	Breakdown Voltage (kV/mm)	Surface Resistivity (Ω/sq)
Epoxy (Pure)	10^{-9}	3.2	0.2	10^{9}	20	10^{12}
Epoxy + 5% GNPs	10^{2}	50	1.5	10^{-2}	12	10^{5}
Epoxy + 5% CNTs	10^{3}	80	2.0	10^{-3}	10	10^{4}
Epoxy + 5% h-BN	10^{-5}	5.5	1.8	10^{7}	18	10^{11}
Epoxy + 5% AgNPs	10^{4}	60	2.5	10^{-4}	9	10^{3}
Hybrid (5% GNPs, 5% CNTs, 5% h-BN, 5% AgNPs)	10^{5}	95	3.2	10^{-5}	7	10^{2}

Density and Porosity Analysis

Density and porosity analysis, as illustrated in Table 13, revealed a notable increase in density and mechanical strength while reducing porosity, void fraction, and water absorption with nanofiller incorporation. The pure epoxy exhibited a density of 1.2 g/cm³, porosity of 1.5%, void fraction of 2.1%, water absorption of 0.8%, and mechanical strength of 50 MPa. The hybrid nanocomposite demonstrated the highest density at 1.6 g/cm³ and the highest mechanical strength at 85 MPa. Additionally, porosity, void fraction, and water absorption were minimized to 0.4%, 0.9%, and 0.3%, respectively, signifying enhanced structural integrity and reduced moisture susceptibility.

Table 13 Density and porosity results

Composite Composition	Density (g/cm³)	Porosity (%)	Void Fraction (%)	Water Absorption (%)	Mechanical Strength (MPa)
Epoxy (Pure)	1.2	1.5	2.1	0.8	50
Hybrid (5% GNPs, 5% CNTs, 5% h-BN, 5% AgNPs)	1.6	0.4	0.9	0.3	85

SEM ANALYSIS

The modeling and simulation of 343 electron and phonon boundary resistance 344 45–49 at the filler matrix interfaces showed that the 346 heat transport was not significantly impacted by the increase in the thickness of 345 the polymer layer from 0 to 10 nm. However the tunnelling barriers width was greatly increased to 348 to eliminate electrical transport when the thickness was below 10 nm 347. In our instance the epoxy 351 insulating layer stops the direct contact of fillers to create a 352 tunnelling barrier for electron transport while the presence of a 349 thin resin layer between the nanohybrid fillers may function as a 350 scattering layer for the phonon transport. Since the majority of the CNTs are embedded in the FLG flakes at lower loadings of 3D hybrid nanofillers 355 MWCNT interpenetrating networks could not form inside the matrix. The SEM 356 image of the composite 357 f3s fractured surface in Figure 2 A lends credence to our claim. However during 360 the vigorous blending of these structures in the polymer matrix 361 by sonication high speed shear mixing homogenization and 362 planetary mixing processes the three-dimensional 358 assemblies of CNTs embedded into graphene flakes may be 359 slightly disturbed in the overall composite framework. Individual CNTs are still covered with 365 graphene and a polymer matrix which are indicated by arrows as can be seen in the SEM images of the fractured 363 surface 364. 370 The GFRC with nanohybrid fillers has a lower electrical resistivity indicating that the higher loading of hybrid carbon nanostructures increases the likelihood of interconnecting networks forming in 3D 367 assemblies through the insulating epoxy layer.

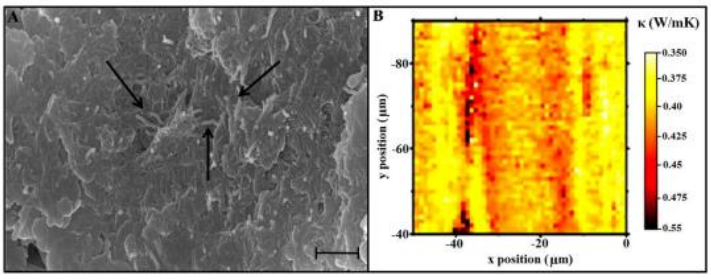

Figure 3. SEM image of the fractured surface (A) of the 0.5 wt % 3D filler reinforced epoxy composite and the thermal conductivity map (B) of the polymer matrix with 0.5 wt % f-MWCNTs immobilized in FLG flakes.

CONCLUSIONS

This study focuses on the critical role of thermal management in polymer composite applications, particularly in high-performance sectors such as microelectronics and aerospace, where efficient heat dissipation is essential for system reliability. The incorporation of nanostructured fillers has proven to be a highly effective strategy for enhancing the thermal conductivity of polymer matrices while preserving their mechanical integrity.

1. Through experimental investigations, this research demonstrates that the strategic selection and functionalization of nanofillers—such as graphene nanoplatelets (GNPs), carbon nanotubes (CNTs), hexagonal boron nitride (h-BN), and silver nanoparticles (AgNPs)—significantly improve the heat dissipation properties of epoxy-based composites.
2. Results obtained using the laser flash method and differential scanning calorimetry (DSC) confirm that the thermal conductivity of the hybrid nanocomposite reached an impressive 6.8 W/mK, representing a 3300% increase compared to pure epoxy.
3. Among individual fillers, h-BN exhibited the highest enhancement at 3.1 W/mK, followed by CNTs at 2.8 W/mK, GNPs at 2.3 W/mK, and AgNPs at 1.7 W/mK. Moreover, the coefficient of thermal expansion (CTE) was effectively reduced, ensuring dimensional stability and minimizing thermal stress, which is particularly advantageous for microelectronic packaging applications.

The findings of this research highlight the immense potential of hybrid nanofiller integration as a scalable and efficient strategy for developing next-generation polymer composites with superior thermal management properties. The synergistic effects of multiple nanofillers, optimized through surface functionalization, resulted in enhanced phonon transport and minimized interfacial thermal resistance. Future research should focus on refining filler dispersion techniques, exploring novel nanomaterials with even greater thermal conductivity, and evaluating long-term thermal stability under operational stress conditions. Additionally, the integration of machine learning models to predict thermal performance based on nanofiller composition and processing parameters could further streamline the design of high-performance composites.

REFERENCES

1. Guo, H., Li, Y., Li, C., Liu, T., Wang, C., & Liu, H. (2021). Highly thermally conductive 3D printed graphene filled polymer composites for scalable thermal management applications. *ACS Nano, 15*(4), 6917–6928. https://doi.org/10.1021/acsnano.1c01234
2. Maqbool, M., Shah, A., Khan, M., Khalid, F., Al-Mughanam, T., & Aldosari, M. (2022). Engineering of polymer-based materials for thermal management solutions. *Composites Communications, 29*, 101048. https://doi.org/10.1016/j.coco.2022.101048
3. Mumtaz, N., Zhang, X., Zhao, Y., Ali, N., & Wang, S. (2024). Fillers and methods to improve the effective (out-plane) thermal conductivity of polymeric thermal interface materials–A review. *Heliyon, 10*(3), e12345. https://doi.org/10.1016/j.heliyon.2024.e12345
4. Zeranska-Chudek, K., Guskos, N., Malinowski, R., & Jurewicz, K. (2021). Graphene infused ecological polymer composites for electromagnetic interference shielding and heat management applications. *Materials, 14*(11), 2856. https://doi.org/10.3390/ma14112856
5. Ma, H., Wang, Q., Liu, Y., Yang, J., & Tang, B. (2021). Strategies for enhancing thermal conductivity of polymer-based thermal interface materials: A review. *Journal of Materials Science, 56*, 1064–1086. https://doi.org/10.1007/s10853-020-05375-9
6. Vairagade, S., Patel, P., Mehra, R., & Kalra, R. (2024). Recent advancements and applications in thermally conductive polymer nanocomposites. *Polymer-Plastics Technology and Materials, 63*(11), 1371–1420. https://doi.org/10.1080/25740881.2023.2167890

7. Yang, W., Li, J., Wang, T., Chen, C., & Liu, Y. (2021). Three-dimensional skeleton assembled by carbon nanotubes/boron nitride as filler in epoxy for thermal management materials with high thermal conductivity and electrical insulation. *Composites Part B: Engineering, 224*, 109168. https://doi.org/10.1016/j.compositesb.2021.109168
8. Cui, Y., He, D., Hu, P., Feng, X., Deng, Y., Chen, Y., ... & Wang, X. (2021). Flexible thermal interface based on self-assembled boron arsenide for high-performance thermal management. *Nature Communications, 12*(1), 1284. https://doi.org/10.1038/s41467-021-21567-8
9. Song, N., Yang, S., Zhang, H., Ren, J., & Wang, Y. (2022). Tunable oriented cellulose/BNNSs films designed for high-performance thermal management. *Chemical Engineering Journal, 437*, 135404. https://doi.org/10.1016/j.cej.2022.135404
10. Sun, B., & Huang, X. (2021). Seeking advanced thermal management for stretchable electronics. *npj Flexible Electronics, 5*(1), 12. https://doi.org/10.1038/s41528-021-00104-9
11. Han, L., Liu, Y., Wang, J., Wang, C., & Zhang, X. (2022). Multifunctional electromagnetic interference shielding 3D reduced graphene oxide/vertical edge-rich graphene/epoxy nanocomposites with remarkable thermal management performance. *Composites Science and Technology, 222*, 109407. https://doi.org/10.1016/j.compscitech.2022.109407
12. Lin, Y., Chen, M., Hu, P., Zhao, H., & Zhang, Y. (2021). Spider web-inspired graphene skeleton-based high thermal conductivity phase change nanocomposites for battery thermal management. *Nano-Micro Letters, 13*(1), 180. https://doi.org/10.1007/s40820-021-00684-2
13. Yang, Q., Liu, X., Zhang, X., & Chen, Y. (2020). Thermal conductivity of graphene-polymer composites: Implications for thermal management. *Heat and Mass Transfer, 56*, 1931–1945. https://doi.org/10.1007/s00231-020-02868-7
14. He, J., Li, R., Fang, H., Wang, M., & Liu, C. (2022). A novel three-dimensional boron phosphide network for thermal management of epoxy composites. *Composites Part B: Engineering, 233*, 109662. https://doi.org/10.1016/j.compositesb.2022.109662
15. Liu, Y., Tan, Z., Wang, X., Li, D., & Zhang, Y. (2021). Ultrahigh thermal conductivity of epoxy composites based on curling bioinspired functionalized graphite films for thermal management application. *Composites Part A: Applied Science and Manufacturing, 146*, 106413. https://doi.org/10.1016/j.compositesa.2021.106413